Ceramics International xxx (xxxx) xxx–xxx

Contents lists available at ScienceDirect

Ceramics International

journal homepage: www.elsevier.com/locate/ceramint

Crystal structure, Raman spectra and microwave dielectric properties of $Li_2Mg_3Ti_{1-x}(Mg_{1/3}Nb_{2/3})_xO_6$ ($0 \le x \le 0.25$) ceramics

Y.K. Yang, H.L. Pan, H.T. Wu*

School of Materials Science and Engineering, University of Jinan, Jinan 250022, China

ARTICLE INFO

Keywords:
$Li_2Mg_3Ti_{1-x}(Mg_{1/3}Nb_{2/3})_xO_6$
Microwave dielectric ceramics
Crystal structure
Raman spectra

ABSTRACT

$Li_2Mg_3Ti_{1-x}(Mg_{1/3}Nb_{2/3})_xO_6$ ($0 \le x \le 0.25$) ceramics were prepared by a conventional solid-state reaction process. Their crystal structures, sintering characteristics, Raman spectra and microwave dielectric properties were then investigated. XRD patterns of the sintered samples indicated that all compositions showed a single phase and the rock-salt structure. As the $(Mg_{1/3}Nb_{2/3})^{4+}$ contents increase, the variations of ε_r values showed a downward trend, which could be explained by the changes of polarizabilities and the shift of Raman vibration modes. $Q{\cdot}f$ values initially increased to a maximum value and then decreased with increasing of x values. In addition, τ_f values decreased almost linearly with the x values, which significantly correlated with the thermal expansion coefficient. Excellent combined microwave dielectric properties with $\varepsilon_r = 14.79$, $Q{\cdot}f = 204{,}900$ GHz and $\tau_f = -18.43$ ppm/°C were obtained for $Li_2Mg_3Ti_{.95}(Mg_{1/3}Nb_{2/3})_{.05}O_6$ ceramic sintered at 1550 °C.

1. Introduction

Over the past few decades, dielectric ceramics or even thin films with excellent properties have been widely used for microwave communication, such as mobile communications, Global Positioning Systems (GPS), Wireless Fidelity (WIFI), Radar systems, etc. [1–3]. Recently, several materials, such as $BaAl_{2-2x}(ZnSi)_xSi_2O_8$, (1-x) $Mg_6Ti_5O_{16}$-x$Ca_{.8}Sr_{.2}TiO_3$, $SrLa[Al_{1-x}(Mg_{.5}Ti_{.5})_x]O_4$, have attracted research interest [4–8]. Generally speaking, these materials are required to possess three performance parameters: appropriate ε_r, high $Q{\cdot}f$ and near-zero τ_f [9,10]. The high Q values can lead to low insertion loss and are important for obtaining the high frequency selectivity of microwave components [11,12]. So, developing microwave dielectric ceramics with high Q values is still a hot research area.

In recent years, $Li_2Mg_3TiO_6$-based materials (Table 1) have been widely investigated because of the ultra-low dielectric loss [13–23]. For instance, Liu et al. reported that $Li_2Mg_3TiO_6$ ceramic had the excellent properties of $\varepsilon_r = 15.2$, $Q{\cdot}f = 152{,}000$ GHz and $\tau_f = -39$ ppm/°C [13,14]. Wu et al. researched the relationships between intrinsic factors and dielectric properties for Li_2O-MgO-BO_2 (B=Ti, Sn, Zr) ceramics [15]. In addition, in order to improve the microwave dielectric properties, divalent cations (Ca^{2+}, Ni^{2+}, Zn^{2+}, Co^{2+} and Mn^{2+}) and quadrivalent cations (Zr^{4+} and Ge^{4+}) were used to displace Mg^{2+} and Ti^{4+} ions, respectively [17–21]. For example, effects of A^{2+} (A = Ca, Ni, Zn and Mn) ions on the phase compositions and properties of $Li_2(Mg_{.95}A_{.05})_3TiO_6$ (A = Ca, Ni, Zn and Mn) ceramics were researched by Zhao et al. [17]. To satisfy the requirements of LTCC, low melting point compounds such as LiF, CuO, V_2O_5 were used to lower the sintering temperature of $Li_2Mg_3TiO_6$ ceramic [13,22–24]. For instance, Fu et al. reported that 2 wt% LiF and 2 wt% CuO additions could reduce the sintering temperature of $Li_2Mg_3TiO_6$ ceramic to 950 °C [24].

Some researchers reported that the substitutions of complex ions could significantly improve the properties [25–27]. For example, Bian et al. reported that 24 at% of $(Mg_{1/3}Nb_{2/3})^{4+}$ could obviously improve the dielectric properties of Li_2TiO_3 ceramic [25]. However, to the best of our knowledge, effects of complex ions on the crystal structures and properties of $Li_2Mg_3TiO_6$ ceramic have not been investigated. On the basis of our previous reports, Ti-O bonds played a major role in influencing properties of $Li_2Mg_3TiO_6$ ceramic [18,22]. So, $(Mg_{1/3}Nb_{2/3})^{4+}$ complex ions were used to replace Ti^{4+} ions and the influences of $(Mg_{1/3}Nb_{2/3})^{4+}$ on the crystal structures, Raman spectra and properties of $Li_2Mg_3Ti_{1-x}(Mg_{1/3}Nb_{2/3})_xO_6$ ($0 \le x \le 0.25$) ceramics were investigated.

2. Experimental procedure

Li_2CO_3 (Aladdin, 99.99%), MgO (Aladdin, 99.99%), Nb_2O_5 (Aladdin, 99.99%) and TiO_2 (Aladdin, 99.9%) powders were used as raw materials to prepare $Li_2Mg_3Ti_{1-x}(Mg_{1/3}Nb_{2/3})_xO_6$ ($0 \le x \le 0.25$) ceramics through the conventional solid-state reaction process. The raw materials were weighed according to the stoichiometric ratio above and ball-milled for 24 h. The slurries were dried in an oven and then

* Corresponding author.
E-mail address: mse_wuht@ujn.edu.cn (H.T. Wu).

https://doi.org/10.1016/j.ceramint.2018.03.184
Received 24 January 2018; Received in revised form 14 March 2018; Accepted 20 March 2018

Table 1
Summarized microwave dielectric properties of $Li_2Mg_3TiO_6$-based ceramics.

Materials	ST[a] (°C)	ε_r	Qf (GHz)	τ_f (ppm/°C)	References
$Li_2Mg_3TiO_6$	1280	15.2	152,000	− 39	[7,8]
$Li_2Mg_3TiO_6$	1320	14.42	153,000	− 11.07	[9]
$Li_2Mg_3TiO_6$	1275	13.6	110,703	− 35.1	[10]
$Li_2(Mg_{.95}Zn_{.05})_3TiO_6$	1275	14.6	158,000	3.23	[11]
$Li_2Mg_{2.88}Ca_{.12}TiO_6$	1280	17.8	102,246	− 0.7	[12]
$Li_2Mg_3TiO_6$	1600	14.3	139,200	− 12.4	[13]
$0.96Li_2Mg_3Ti_{.9}Ge_{.1}O_6$ − $0.04CaTiO_3$	1180	14.9	68,900	− 3.5	[14]
$Li_2Mg_3TiO_6$	1500	14.97	125,300	− 24.33	[15]
$Li_2Mg_3TiO_6$ + 4% LiF	950	16.2	131,000	− 44	[7]
$0.9Li_2Mg_3TiO_6$ − $0.1SrTiO_3$ + 4% LiF	900	19.5	64,290	6.5	[16]
$0.8Li_2Mg_3TiO_6$ − $0.2Ca_{.8}Sr_{.2}TiO_3$ + 4% LiF	800	18.8	48,200	0.3	[17]
$Li_2Mg_3TiO_6$ + 2 wt% LiF + 2 wt% CuO	950	15.7	70,100	− 43	[18]
$Li_2Mg_3Ti_{.95}(Mg_{1/3}Nb_{2/3})_{.05}O_6$	1550	14.79	204,900	− 18.43	This work

[a] ST: sintering temperatures.

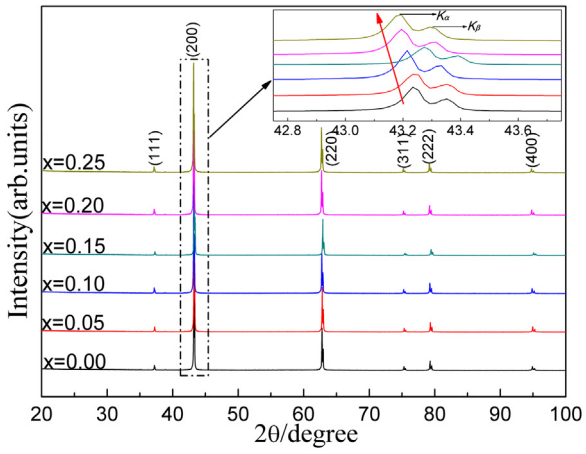

Fig. 1. XRD patterns of $Li_2Mg_3Ti_{1-x}(Mg_{1/3}Nb_{2/3})_xO_6$ ($0 \le x \le 0.25$) ceramics sintered at 1550 °C.

calcined at 1000 °C for 4 h. The calcined powders were re-ground for 24 h and dried again. After dried, the powders were mixed with 8 wt% paraffin and pressed into cylinders (about 10 mm in diameter and about 5 mm in height). These cylinders were preheated to 500 °C to remove the paraffin and then sintered at 1400–1600 °C in sealed platinum crucibles.

Archimede's method was used to measure the apparent densities of sintered samples. Crystal structures of the specimens were identified by X-ray diffraction (XRD, D/MAX-B, Rigaku Co., Japan) with Cu K_α radiation. Rietveld refinement was operated to research the lattice parameters of $Li_2Mg_3Ti_{1-x}(Mg_{1/3}Nb_{2/3})_xO_6$ ($0 \le x \le 0.25$) ceramics using Fullprof software [28]. Raman spectra were recorded by the Raman spectrometer (Lob RAM HR Evolution, HORIBA Jo bin Yvon S.A.S.). Micro-structures were observed by a scanning electron microscopy (SEM, Model JEOL JEM-2010, FEI Co., Japan). Microwave dielectric properties were measured at 8–12 GHz using a network analyzer (N5234A, Agilent Co., American). ε_r and Qf values were measured according to Hakki-Coleman method [29] and cavity method [30], respectively. τ_f values were measured and calculated by Eq. (1).

$$\tau_f = \frac{f_2 - f_1}{f_1(85 - 25)} \quad (1)$$

where f_1 and f_2 are the resonant frequency at the temperature of 25 °C and 85 °C, respectively.

3. Results and discussion

3.1. Crystal structure analysis

Fig. 1 presents XRD patterns of $Li_2Mg_3Ti_{1-x}(Mg_{1/3}Nb_{2/3})_xO_6$ ($0 \le x \le 0.25$) ceramics sintered at 1550 °C. According to the standard PDF card of $Li_2Mg_3SnO_6$ (JCPDS PDF#39–0932), all the diffraction peaks can be indexed as the rock-salt structure with Fm-3 m (No. 225) space group, indicating that $(Mg_{1/3}Nb_{2/3})^{4+}$ can be dissolved into the crystal lattice of $Li_2Mg_3TiO_6$ to form a solid solution. It can been discovered that all peaks, such as (200) peak, slightly shift to the lower angles with the increase of $(Mg_{1/3}Nb_{2/3})^{4+}$ contents from 0 to 0.25, which can be explained by the substitution of larger $(Mg_{1/3}Nb_{2/3})^{4+}$ ion (0.67 Å) for Ti^{4+} ion (0.604 Å) and indicates the increase of the cell volumes. Refinement patterns of $Li_2Mg_3Ti_{1-x}(Mg_{1/3}Nb_{2/3})_xO_6$ ($0 \le x \le 0.25$) samples are shown in Fig. 2. $LiFeO_2$ was used as the initial model for Rietveld refinement of $Li_2Mg_3Ti_{1-x}(Mg_{1/3}Nb_{2/3})_xO_6$ ($0 \le x \le 0.25$) ceramics [31]. It can be found that the calculated patterns match well with the measured ones for all the compositions. The lattice parameters, cell volumes and reliability factors of R_p values, R_{wp} values and χ^2 values are shown in Table 2. With the increase of x values from 0 to 0.25, the cell volumes increase from 73.1444 $Å^3$ to 73.7425 $Å^3$, which agrees well with the results of Fig. 1.

3.2. Raman spectra analysis

Raman spectra can reflect the relationships between lattice vibration modes and resonant patterns, and they also can be used to study the relationships between the structures and properties for solid materials [32]. Fig. 3 exhibits Raman spectra of $Li_2Mg_3Ti_{1-x}(Mg_{1/3}Nb_{2/3})_xO_6$ ($0 \le x \le 0.25$) compounds in the wave number range 50–1200 cm^{-1}, which shows that the spectra profiles are similar to each other. Based on the previous report, the Raman vibrational modes of 185 cm^{-1}, 397 cm^{-1} and 730 cm^{-1} are the characteristic modes of a rock salt structure [33]. In this work, A (about 185 cm^{-1}) and B (about 397 cm^{-1}) vibration modes have no obvious change, while C (about 730 cm^{-1}) vibration mode shows an obviously deviation. The results of C vibration mode are shown in Table 3, which can be used to explain the change of ε_r values.

3.3. Sintering characteristics and micro-morphology

Fig. 4(a) shows the apparent densities of $Li_2Mg_3Ti_{1-x}(Mg_{1/3}Nb_{2/3})_xO_6$ ($0 \le x \le 0.25$) sintered at 1400–1600 °C. It can be found that apparent densities initially increase to the maximum values from 1400 °C to 1550 °C and then decrease from 1550 °C to 1600 °C. The maximum apparent densities are obtained at 1550 °C for different components and the apparent densities gradually increase with the increase of $(Mg_{1/3}Nb_{2/3})^{4+}$ contents. For example, apparent densities gradually increase from 3.26 g/cm^3 to 3.40 g/cm^3 for $Li_2Mg_3Ti_{1-x}(Mg_{1/3}Nb_{2/3})_xO_6$ ($0 \le x \le 0.25$) sintered at 1550 °C. On the basis of atomic weight [34] and lattice parameter, the relative densities are calculation and the result is shown in Fig. 4(b). It can be found that relative densities show a similar trend to apparent densities. For different X values, the maximum relative densities about 93.75–95.86% are obtained at the sintering temperature of 1550 °C.Micro-structures of $Li_2Mg_3Ti_{1-x}(Mg_{1/3}Nb_{2/3})_xO_6$ ($0 \le x \le 0.25$) sintered at 1550 °C are demonstrated in Fig. 5. As the $(Mg_{1/3}Nb_{2/3})^{4+}$ contents increase from 0 to 0.25, the grain sizes exhibit no significant change. The grains exhibit homogeneous state and the average grain size is about 65 μm. It can be concluded that dense micro-structures can be obtained of $Li_2Mg_3Ti_{1-x}(Mg_{1/3}Nb_{2/3})_xO_6$ ($0 \le x \le 0.25$) ceramics sintered at 1550 °C, which agrees with the results of apparent densities.